Accepted Manuscript

Hybrid compounds from chalcone and 1,2-benzothiazine pharmacophores as selective inhibitors of alkaline phosphatase isozymes

Adnan Ashraf, Syeda Abida Ejaz, Shafiq Ur Rahman, Waseeq Ahmad Siddiqui, Muhammad Nadeem Arshad, Joanna Lecka, Jean Sévigny, Mohie E. Moustafa Zayed, Abdullah M. Asiri, Jamshed Iqbal, Christian G. Hartinger, Muhammad Hanif

PII: S0223-5234(18)30841-9

DOI: 10.1016/j.ejmech.2018.09.063

Reference: EJMECH 10774

To appear in: *European Journal of Medicinal Chemistry*

Received Date: 27 June 2018

Revised Date: 17 September 2018

Accepted Date: 25 September 2018

Please cite this article as: A. Ashraf, S.A. Ejaz, S.U. Rahman, W.A. Siddiqui, M.N. Arshad, J. Lecka, J. Sévigny, M.E. Moustafa Zayed, A.M. Asiri, J. Iqbal, C.G. Hartinger, M. Hanif, Hybrid compounds from chalcone and 1,2-benzothiazine pharmacophores as selective inhibitors of alkaline phosphatase isozymes, *European Journal of Medicinal Chemistry* (2018), doi: https://doi.org/10.1016/j.ejmech.2018.09.063.

Graphical Abstract

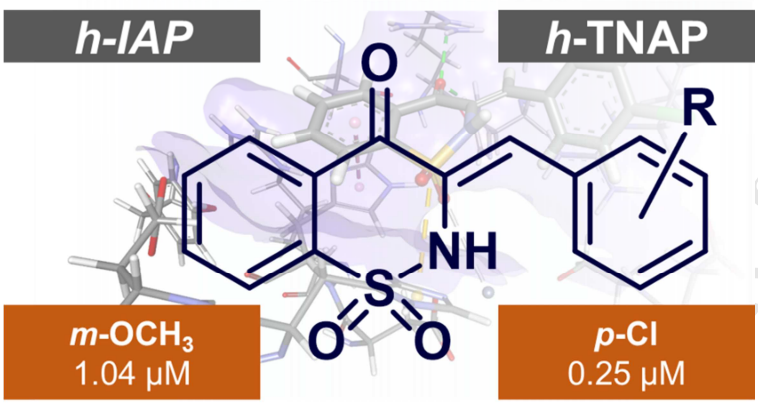

Hybrid Compounds from Chalcone and 1,2-Benzothiazine Pharmacophores as Selective Inhibitors of Alkaline Phosphatase Isozymes

Adnan Ashraf,[a,b] Syeda Abida Ejaz,[c] Shafiq Ur Rahman,[c] Waseeq Ahmad Siddiqui,[b]* Muhammad Nadeem Arshad,[d,e] Joanna Lecka,[f,g] Jean Sévigny,[f,g] Mohie E. Moustafa Zayed,[d,e] Abdullah M. Asiri,[d,e] Jamshed Iqbal,[c] Christian G. Hartinger,[a] Muhammad Hanif[a]*

[a] School of Chemical Sciences, University of Auckland, Private Bag 92019, Auckland 1142, New Zealand

[b] Department of Chemistry, University of Sargodha, Sargodha 40100, Pakistan

[c] Centre for Advanced Drug Research, COMSATS University of Islamabad, Abbottabad Campus, Abbottabad 22060, Pakistan

[d] Department of Chemistry, Faculty of Science, King Abdul Aziz University, P.O. Box 80203, Jeddah 21589, Saudi Arabia

[e] Centre of Excellence for Advanced Materials Research (CEAMR), King Abdul Aziz University, P.O.Box 80203, Jeddah 21589, Saudi Arabia

[f] Département de microbiologie-infectiologie et d'immunologie, Faculté de Médecine, Université Laval, Québec, QC, G1V 0A6, Canada

[g] Centre de Recherche du CHU de Québec – Université Laval, Québec, QC, G1V 4G2, Canada

* School of Chemical Sciences, University of Auckland, Private Bag 92019, Auckland 1142, New Zealand.

E-mail: m.hanif@auckland.ac.nz; Fax: (+64)9 373 7599 ext 86833

Department of Chemistry, University of Sargodha, Sargodha 40100, Pakistan.

Email: waseeq.ahmad@uos.edu.pk

ABSTRACT

Chalcones and 1,2-benzothiazines are two important classes of bioactive compounds, each scaffold endowed with diverse pharmacological activities. Combining both of these pharmacophores in a single molecule was aimed to yield multi-modal agents. Herein, we report a series of hybrid compounds **3a**–**3o** derived from chalcones and 1,2-benzothiazine cores. They were synthesized from commercially available sodium saccharin, and the resulting 1,2-benzothiazine-derived ketone was then condensed with aromatic aldehydes in an aldol condensation to obtain the respective chalcones. The compounds were characterized using different analytical techniques including FT-IR, NMR spectroscopy, mass spectrometry and X-ray crystallography. Some synthesized chalcones revealed potent and/or selective inhibitory properties towards alkaline phosphatase isozymes transiently expressed in COS-7 cells. A detailed structure-activity and selectivity study was carried out with regard to the effect of different substituents at *ortho*-, *meta*- and *para*-positions of the phenyl residue. Compound **3c** was the most effective human intestinal alkaline phosphatase (*h*-IAP) inhibitor (IC_{50} value of 1.04 μM), while it was not active against human tissue non-specific alkaline phosphatase (*h*-TNAP) isozyme. In contrast, **3i** was a selective inhibitor of *h*-TNAP with IC_{50} values of 0.25 ± 0.01 μM. The possible binding interactions of the most effective inhibitors of *h*-TNAP and *h*-IAP were obtained from molecular docking studies.

Keywords

Chalcone; 1,2-benzothiazine; enzyme inhibition; alkaline phosphatase; aldol condensation.

INTRODUCTION

Alkaline phosphatases (APs, E.C. 3.1.3.1) are membrane-bound metalloenzymes which have an active site facing the extracellular space [1]. They hydrolyze phosphate monoesters and are involved in several cellular events including protein phosphorylation, cell growth, and apoptosis. Based on their tissue distribution, APs are classified into four isozymes; tissue specific alkaline phosphatase including placental (PLAP), germ cell (GCAP), intestinal (IAP) and tissue non-specific alkaline phosphatase (TNAP) [2-4]. TNAP is expressed in various tissues through all the stages of development. In bone tissue, it is associated with the hydrolysis of pyrophosphate. By maintaining an optimum level of pyrophosphate, TNAP maintains proper bone mineralization [5]. According to recent reports, TNAP overexpression is observed in renal and bone diseases [1]. Among tissue-specific APs, IAP is responsible for regulating bicarbonate secretion, detoxification of bacterial lipopolysaccharides, lipid intestinal absorption as well as the maintenance of the pH value at the duodenal surface [6].

APs have been reported to be overexpressed in solid and metastasized tumors including breast, esophageal, liver, colon, intestinal, prostate and ovarian cancer [7]. The elevated level of TNAP and IAP in many cancers and other pathologies makes them an interesting molecular target in drug discovery [8, 9]. There is an increasing interest in the design of effective and selective inhibitors of AP isozymes [10]. In recent years, different inhibitors of APs based on diaryl sulfonamides, coumarin sulfonates, triazole, chalcones and chromones have been reported [11-16]. Some compounds were found to be effective inhibitors of TNAP and IAP but most of them inhibited APs non-selectively [11-15].

With the aim to find selective inhibitors of APs, we report the synthesis of a series of compounds based on two pharmaceutically-active scaffolds, namely chalcones and benzothiazines. The chalcone scaffold is considered a privileged structure and represents the key structural motif in a plethora of bioactive synthetic and natural compounds, widely distributed across fruits, vegetables, and other plants [17]. Chalcones are the precursors in the biosynthesis of flavonoids in plants and the core of many biologically-active hybrid natural compounds such as coumarin-chalcone hybrids [18]. Chalcones and their derivatives have pharmacological properties such as anticancer, antioxidative, antibacterial, antiviral, insecticidal, antiprotozoal,

antiulcer and immunosuppressive activity [17, 19, 20], and several examples have been approved for clinical use (Chart 1). They exert their cytotoxic effects through a number of mechanisms, such as inhibition of receptor tyrosine kinases including the epidermal growth factor receptor (EGFR) [21], and the vascular endothelial growth factor receptor 2 (VEGFR-2) [21, 22]. They have also been shown to interfere with the nuclear factor NF-κB signaling pathway [23], tubulin polymerization [24], thioredoxin reductase (TrxR) and dihydrofolate reductase (DHFR) [25, 26].

Benzothiazines represent another interesting scaffold. Their structures feature a non-aromatic heterocyclic core and an all-carbon aromatic fragment [27]. They are key components of important pharmaceuticals such as anti-inflammatory drugs (Chart 1) [28, 29], and have been extensively studied for biological applications including as antibacterial [30], antiviral [31, 32], antifungal [33], antioxidant [34, 35], and antitumor agents [36, 37]. Several recent studies highlighted their role as potent inhibitors of 11β-hydroxysteroid dehydrogenase type 1 (11β-HSD1) [38], calpain I [39], and aldose reductase [40-42]. These diverse biological applications of 1,2-benzothiazines have attracted an increasing interest in the structural modification of this scaffold [43-46].

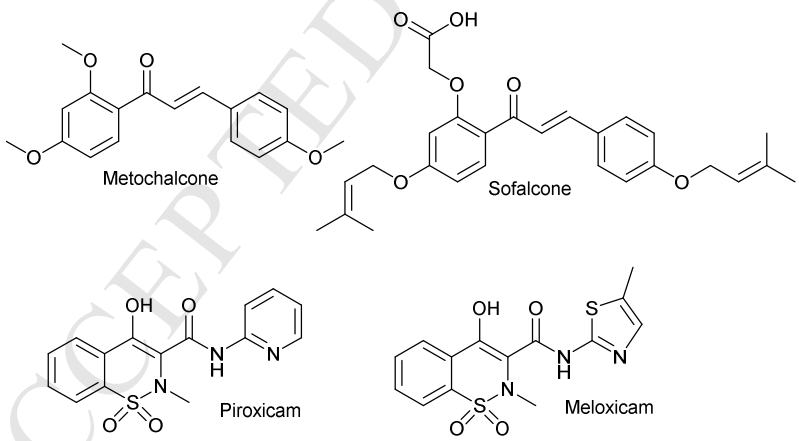

Chart 1. Chemical structures of the clinical approved chalcone-based drugs metochalcone and sofalcone, and the 1,2-benzothiazine-derived anti-inflammatory agents piroxicam and meloxicam.

In our continued interest in developing 1,2-benzothiazine and sulfonamide heterocyclic compounds [29, 37, 47], we report a series of hybrid compounds based on the 1,2-benzothiazine core and a chalcone scaffold to harvest the biological properties of both motifs. Several compounds revealed to be either potent and/or

specific inhibitor of APs. This evaluation was complemented with molecular docking studies of the molecules with the highest potential for specificity and potency to further understand the mechanisms of their interaction with the AP enzymes.

Results and discussion

Synthesis and characterization

We prepared compounds **5a–5o** starting from methyl 4-hydroxy-2*H*,1,2-benzothiazine-3-carboxylate 1,1-dioxide **3**, which was obtained from sodium saccharin **1** in a reaction with methyl chloroacetate under mild conditions. A Gabriel–Colman type ring expansion converted the 5-membered isothiazole ring in **2** to a 6-membered thiazine ring to give **3**. Hydrolysis and decarboxylation of **3** in refluxing concentrated hydrochloric acid yielded 1,1-dioxo-2*H*-1,2-benzothiazine-4-one **4** [48-51]. An aldol condensation of **4** with the respective aldehydes was carried out in alkaline solution at ambient temperature. After completion of the reaction, the mixture was acidified which resulted in the formation of yellow precipitates. The solids formed were recrystallized from methanol to obtain the pure compounds **5a**–**5o**.The preparation of **5a** has been reported by Zinnes and co-workers under relatively harsh conditions using sodium borohydride or sodium hydride at temperatures as low as -20 ℃ [48, 49].

The compounds were characterized by FT-IR and NMR spectroscopy, high resolution mass spectrometry and X-rays crystallographic techniques. In the IR spectra of **5a**–**5o**, the NH signal of the thiazine ring appeared in the range of 3230–3078 cm^{-1} while this signal was present at 3269 cm^{-1} for precursor **4**. The α,β-unsaturated carbonyl stretching vibrations were detected in the range of 1689–1651 cm^{-1}. A new alkene group (C=C) stretching frequency appeared in the range of 1600–1581 cm^{-1}, indicative of the formation of the desired product. The sulfonyl group asymmetric and symmetric stretching frequencies appeared in the range of 1375–1290 cm^{-1} and 1174–1156 cm^{-1}, respectively.

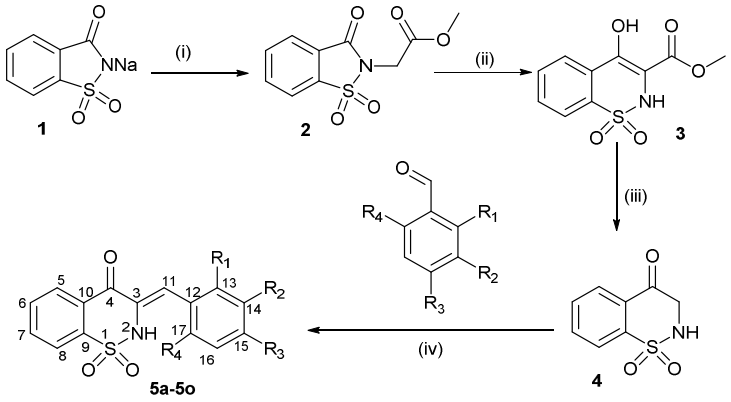

5a, $R_1 = R_2 = R_3 = R_4 = H$
5b, $R_1 = OCH_3$, $R_2 = R_3 = R_4 = H$
5c, $R_2 = OCH_3$, $R_1 = R_3 = R_4 = H$
5d, $R_3 = OCH_3$, $R_1 = R_2 = R_4 = H$
5e, $R_1 = Br$, $R_2 = R_3 = R_4 = H$
5f, $R_2 = Br$, $R_1 = R_3 = R_4 = H$
5g, $R_3 = Br$, $R_1 = R_2 = R_4 = H$
5h, $R_2 = Cl$, $R_1 = R_3 = R_4 = H$
5i, $R_3 = Cl$, $R_1 = R_2 = R_4 = H$
5j, $R_1 = R_3 = Cl$, $R_2 = R_4 = H$
5k, $R_2 = F$, $R_1 = R_3 = R_4 = H$
5l, $R_3 = F$, $R_1 = R_2 = R_4 = H$
5m, $R_1 = R_3 = F$, $R_2 = R_4 = H$
5n, $R_1 = CH_3$, $R_2 = R_3 = R_4 = H$
5o, $R_2 = OH$, $R_1 = R_3 = R_4 = H$

Scheme 1. Synthesis of the hybrid compounds **5a**–**5o** based on the 1,2-benzothiazine and chalcone scaffolds; i) $ClCH_2COOCH_3$, DMF, reflux; ii) NaOMe, MeOH, 60 ℃; iii) HCl, re flux; iv) NaOH, MeOH/H_2O, 25 ℃.

The ^1H NMR spectra of **5a**–**5o** revealed a characteristic singlet for the vinylic hydrogen which appeared between 7.77 and 7.62 ppm and was assigned to H-11. The CH_2 signal at 4.29 ppm in precursor ketone **4** was absent in **5a**–**5o**. The most downfield signal was a singlet in the range 11.03–10.48 ppm which was assigned to H-2 (NH). The proton signals for the benzothiazine aromatic ring were not impacted by the introduction of substituents R_1–R_4. The aromatic proton signals from the benzaldehyde fragment (H-13 to H-17) however appeared between 8.19 and 6.92 ppm. These signals were shifted in the presence of different electron-donating and -withdrawing groups attached to the aromatic ring system.

In the $^{13}C\{^1H\}$ NMR spectra, the most deshielded carbon atoms C-4 and C-3 of benzothiazine were found around 180 and 141 ppm in all compounds. The detection of C-3 as quaternary carbon indicated the formation of the chalcones.

The chemical shift of the C-11 signals depends upon the substituents attached to the ring. Electron donating groups, including methoxy, methyl and hydroxyl attached to the benzaldehyde ring in **5b–5d**, **5n** and **5o**, caused an upfield shift of C-11, whereas electron withdrawing fluoro, chloro and bromo in compounds **5d–5m** led to a deshielding effect. In **5k**, **5l** and **5m**, the fluorine couple with neighbouring carbon atoms, with coupling constant $^1J_{(C,F)}$ = 252 Hz in case of **5l** (Figure S27 and S29).

The synthesized compounds were also analyzed by high resolution ESI-MS in positive ion mode. All mass spectra featured the pseudomolecular $[M + H]^+$ or $[M + Na]^+$ ions (100%) with very well matched calculated and observed *m/z* values.

The molecular structures of **5d**, **5h**, and **5n** were determined by X-ray diffraction analysis and all three compounds demonstrated (*Z*)-configuration. The crystallographic data is provided in Table S1. The tetrahedral geometry found for the sulfur atom was distorted with O=S=O angles of about 120° (Figure 1 and S1) [52-54]. The substituted aromatic rings are oriented at dihedral angles of 10.832(1)°, 18.832(6)° and 13.128(5)° with respect to the thiaz ine ring in **5h**, **5n** and **5d**, respectively. The puckering parameters for the rings in all three molecules were determined, and the thiazine rings were found to be non-planar.

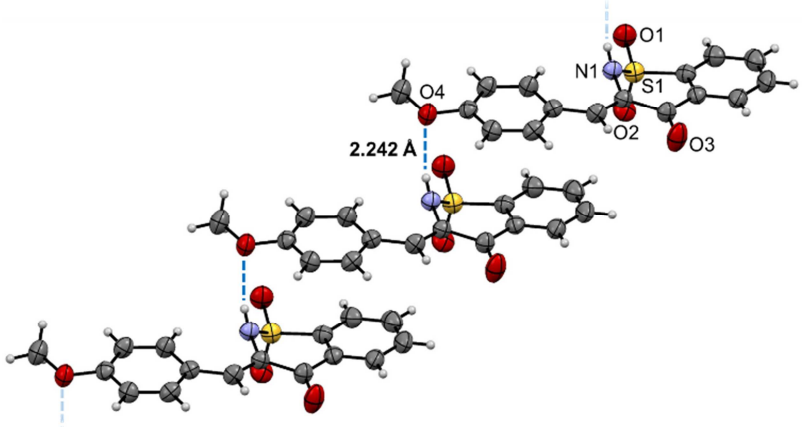

Figure 1. Molecular structure of **5d** drawn at 50% probability level. Intermolecular H bonds are shown between the hydrogen of NH in position 2 and the oxygen of the methoxy group.

Intermolecular hydrogen bonding was observed in all three molecules (Figure 1 and S1). In **5d** intermolecular hydrogen bonds were formed between the NH hydrogen and O4 of the methoxy group with N1-H···O4 distances of 2.242 Å (Figure 2). The N-H···O interaction causes formation of an extended network of H bond-bridged molecules (Figure 1). While in **5h** and **5n** intermolecular hydrogen bonds were present between the N1H hydrogen and carbonyl oxygen O3 with N1H···O3 distances of 2.074(3) and 2.000(3) Å, respectively (Figure 1 and S1). In **5h** and **5n**, N1H···O interactions connect the molecules to generate chain structures. The bond lengths and bond angles were in the normal range (Figure 2 and S1) [52-54]. In all three structures the C=O bond lengths were between 1.229(3) and 1.217(13) Å, while the C=C distances were in the range of 1.342(3)-1.316(17) Å.

Enzyme inhibitory activity

The 1,2-benzothiazine-based chalcones **5a–5o** were evaluated for alkaline phosphatase inhibitory activity against selected isozymes of alkaline phosphatase, *i.e.*, *h*-TNAP and *h*-IAP. The introduction of substituents on the phenyl ring of **5a** resulted in promising inhibitory effects on the selected isozymes of alkaline phosphatase; *h*-TNAP and *h*-IAP. It appeared that *para*-substituted derivatives exhibited more promising inhibitory effects on *h*-TNAP while the *ortho*- and *meta*-substituted derivatives exhibited more selective inhibition of *h*-IAP. Derivative **5a**, having an unsubstituted phenyl ring, showed inhibition of *h*-TNAP with an IC_{50} value of 0.66 µM (Table 1). The most potent inhibitor of *h*-TNAP was **5i** bearing chloro group at *para* position with an IC_{50} value of 0.25 µM. It exhibited approximately 80 fold greater inhibition compared to the standard reference compound levamisole (IC_{50} = 20.2 µM) [55].

Table 1. *In vitro* alkaline phosphatase (*h*-TNAP and *h*-IAP) inhibitory activities of **5a**–**5o** expressed as IC_{50} (μM) and their cytotoxic activities against HeLa cervical carcinoma cells after treatment with 100 μM of the compound.

Compounds	*h*-TNAP IC_{50} [b] / μM	*h*-IAP IC_{50} [b] / μM	selectivity index [a]	% growth inhibition
5a	0.66 ± 0.02	1.78 ± 0.22	0.4	19 ± 2
5b	2.59 ± 0.22	1.24 ± 0.42	2.1	17 ± 0.3
5c	> 200 [b]	1.04 ± 0.11	> 190	39 ± 3
5d	4.04 ± 0.21	1.53 ± 0.11	2.6	11 ± 2
5e	> 200 [b]	7.43 ± 0.26	> 1	53 ± 1
5f	> 200 [b]	2.55 ± 0.72	> 26	65 ± 1
5g	1.43 ± 0.13	3.69 ± 0.51	0.4	59 ± 3
5h	> 200 [b]	3.77 ± 0.38	> 50	64 ± 1
5i	0.25 ± 0.01	4.35 ± 0.39	0.1	55 ± 3
5j	> 200 [b]	4.96 ± 0.31	> 53	59 ± 4
5k	3.19 ± 0.74	9.93 ± 1.03	0.3	53 ± 2
5l	1.35 ± 0.11	3.06 ± 0.35	0.4	41 ± 6
5m	1.53 ± 0.34	10.6 ± 1.2	0.1	17 ± 1
5n	2.36 ± 0.19	3.75 ± 0.38	0.6	7.0 ± 0.9
5o	3.57 ± 0.24	1.21 ± 0.13	3.0	15 ± 2
levamisole	20.2 ± 1.9	> 200 [c]	< 0.1	–
L-phenylalanine	> 200 [c]	100 ± 3	> 2	–
cisplatin	–	–	–	89 ± 2

[a] a selectivity index > 1 indicates selectivity for *h*-IAP and < 1 for *h*-TNAP; [b] mean ± SEM (Standard error mean; n = 3); [c] highest conc. used.

The substitution of a fluoro with a chloro atom at *para* position in **5l**, resulted in relatively reduced inhibitory effects (IC_{50} = 1.35 μM) on *h*-TNAP as compared to **5i**, but it was still more selective for *h*-TNAP. The derivatives **5c**, **5e**, **5f**, **5h** and **5j** exhibited less than 50% inhibitory activity against *h*-TNAP isozyme at the highest used concentration of 200 μM and therefore these derivatives were not selected for the evaluation of their IC_{50} values.

All compounds showed moderate to excellent inhibitory effects on *h*-IAP depending on the type and position of the attached substituent. The derivatives having electron donating group (**5b**, **5c**, **5d** and **5o**) exhibited greater inhibitory potential as compared to other derivatives with unsubstituted phenyl ring **5a** or carrying electron

withdrawing group substitution. Compound **5c** (IC_{50} = 1.04 ± 0.11 µM) exhibited the highest selectivity and strongest inhibitory effects on *h*-IAP, while **5i** was the most potent and selective *h*-TNAP inhibitor of the series of compounds investigated.

For the investigation of the kinetics of the enzyme inhibition of the most potent inhibitors **5c** against *h*-IAP and **5i** against *h*-TNAP, double reciprocal plots of initial velocity and substrate CDP-Star® concentrations were prepared. The enzyme kinetic studies were performed for **5i** and **5c** at different compound concentrations (Figures 2 and S3). The selective inhibitor of *h*-IAP, *i.e.*, **5c**, exhibited competitive inhibition of this isozyme as the intercept of the curves is on the y-axis for uninhibited and inhibited enzymes (Figure 2). In contrast, the selective *h*-TNAP inhibitor **5i** exhibited non-competitive inhibition (Figure S3).

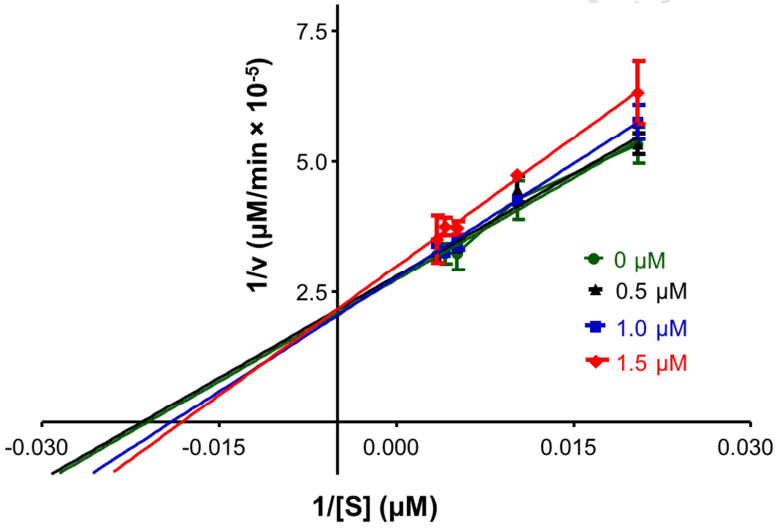

Figure 2. Double reciprocal plot of the inhibition kinetics of *h*-IAP by the most potent compound **5c**, showing competitive inhibition.

Molecular Docking Studies

Molecular docking studies were carried out to identify plausible binding interactions of the most potent derivatives against *h*-IAP and *h*-TNAP, *i.e.*, **5c** and **5i**, respectively, with the modeled structures of the respective isozymes. For validation of the docking studies, the standard inhibitors levamisole and L-phenylalanine, which were also used in the inhibition assays for *h*-TNAP and *h*-IAP, respectively, were docked in the active pockets of the enzymes.

Docking studies of **5c** into the active pocket of *h*-IAP revealed several interactions (Figure 3). One of the oxygen atoms of the sulfur dioxide group was involved in H bonds with Arg166 and His432 and the sulfur atom is involved in a π-interaction with His432, while the other oxygen atom demonstrated binding to the zinc(II) ion within the active site of *h*-IAP (Figure 3). The chalcone carbonyl oxygen formed two H bonds with Arg166 and Gln108. The benzene ring adjacent to the thiazine ring was involved in a π-interaction with Thr431. Notably, when docking **5i** into *h*-IAP, different interactions were observed. These included coordination of the sulfoxide oxygen atoms to Zn and π-interactions with His320 as well as between chlorophenyl group and His432 and Phe107, while no strong hydrogen bonds were observed (Figure S4).

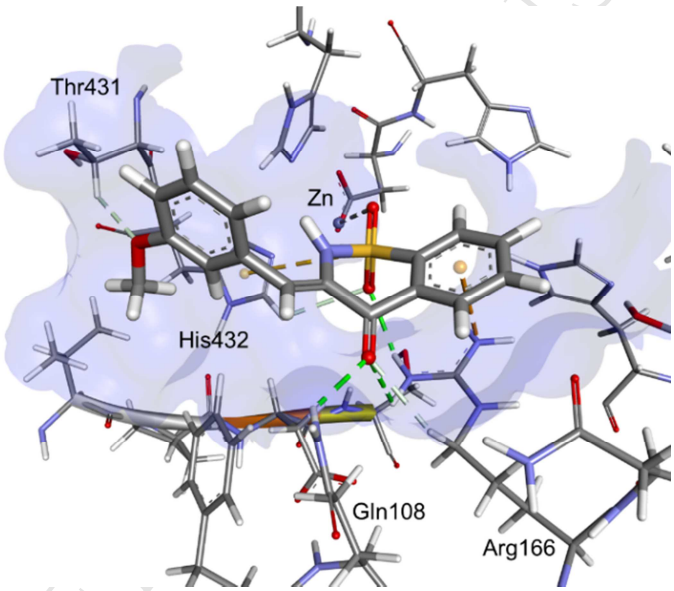

Figure 3. Docking study of **5c** into the active site of *h*-IAP. Hydrogen bonds and π-interactions between compound and amino acid residues are shown as dashed lines.

The docking of **5i** with *h*-TNAP revealed H bond formation between the chalcone oxygen atom and His154 and Arg151, while π-interactions were formed between the condensed aromatic system of **5i** and His321 (Figure 4). His324 was involved in a π-interaction with the sulfur atom and an oxygen of the sulfur dioxide moiety coordinated to the Zn in the active site (Figure 4). Compound **5c** formed very different interactions with *h*-TNAP involving interactions between an SO_2 oxygen atom and the two adjacent His residues, and π-interactions with Arg167 and His321 (Figure S5), while H bonds were absent.

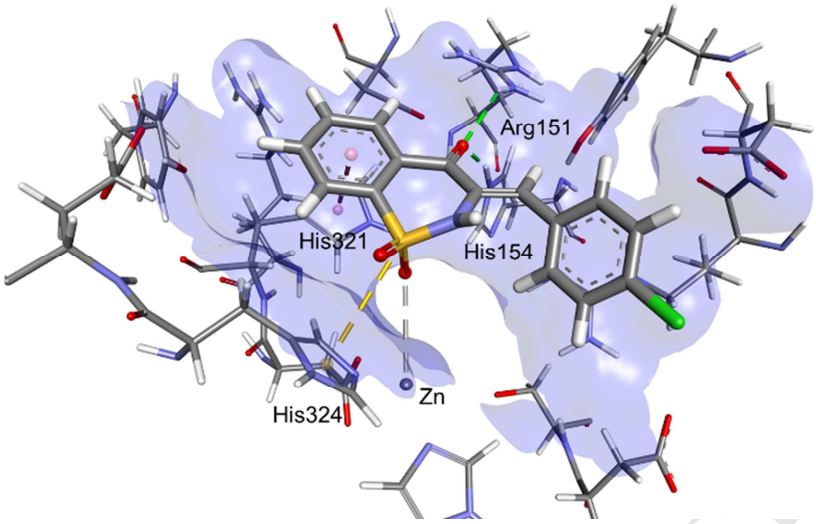

Figure 4. Docking study of **5i** into the active site of *h*-TNAP. Hydrogen bonds and π-interactions between compound and amino acid residues are shown as dashed lines.

In vitro cytotoxicity against HeLa cervical carcinoma cells

The cytotoxic activity of **5a**–**5o** against cervical carcinoma cells HeLa was evaluated by means of the MTT [3-(4,5-dimethylthiazol-2-yl)-2,5-diphenyltetrazolium bromide] assay. The percentage inhibition of all the derivatives was investigated at 100 µM (Table 1). Cisplatin was used as a positive control and it showed a 89% growth inhibition at the same concentration level (100 µM). As cisplatin is known to be highly cytotoxic, it is not surprising that most of the derivatives showed lower antiproliferative activity towards the cancer cells than cisplatin. Compounds **5e**–**5k** were the most cytotoxic derivatives with 53 to 65% growth inhibition of HeLa cells. In contrast, **5a**, **5b**, **5d** and **5m**–**5o** exhibited very low toxicity towards HeLa cells.

Conclusions

A series of heterocyclic compounds **5a**–**5o** based on chalcone and 1,2-benzothiazine scaffolds was developed by condensation of different aldehydes with the 1,2-benzothiazine core. All compounds were evaluated for their inhibitory potential against the alkaline phosphatase isoforms *h*-TNAP and *h*-IAP and the latter was more responsive to inhibition by the compound class. The positioning and nature of the functional groups impacted the activity as well as the isozyme selectivity of the compounds. All the *para*-substituted compounds showed activity in

the low μM concentration range against both isoforms but with limited selectivity. The notable exception is the *p*-Cl derivative **5i** which was the most potent inhibitor of *h*-TNAP at 0.25 μM and a selective index of 0.1. For the *meta*-substituted compounds **5c**, **5f**, and **5h** high selectivity for *h*-IAP was observed with **5c** being most potent (1.04 μM). Molecular docking studies revealed different interaction modes for compounds **5c** and **5i** within the active site of the two AP isoforms for *h*-IAP and *h*-TNAP, respectively. While the compounds interacted with the Zn ions in both isoforms, they lacked the formation of H bonds with the isoform they showed lower activity in. Therefore, these observations are in line with the data collected in the enzyme inhibition studies and support the high selectivity of **5c** for *h*-IAP over *h*-TNAP and vice versa for **5i**.

Conflicts of interest

There are no conflicts to declare.

Acknowledgments

We thank the Higher Education Commission of Pakistan for research project NRPU 20-1582 and indigenous/IRSIP scholarship (A.A.). J. I. is thankful to the Organization for the Prohibition of Chemical Weapons (OPCW), The Hague, The Netherlands and Higher Education Commission of Pakistan for the financial support through Project No. 20–3733/NRPU/R&D/14/520. J.S. received support from the Canadian Institutes of Health Research (CIHR) and was the recipient of a “Chercheur National” research award from the Fonds de recherche du Québec – Santé (FRQS).

EXPERIMENTAL SECTION

Materials and Methods

All the reactions were carried out at ambient temperature. All the chemicals were of analytical grade and used without further purification. Food grade sodium saccharin (cooko) was purchased from a local market. Chloroacetic acid, sodium, benzaldehyde, 2-methoxy benzaldehyde, 3-methoxy benzaldehyde, 4-methoxy benzaldehyde, 2-bromo benzaldehyde, 3-bromo benzaldehyde, 4-chloro benzaldehyde, 2,4-dichloro benzaldehyde, 2- methyl benzaldehyde and 2-hydroxy benzaldehyde were purchased from Scharlau (United Kingdom) and 2-bromo benzaldehyde, 4-bromo benzaldehyde, 3-chloro benzaldehyde, 3-fluoro benzaldehyde, 4-fluoro benzadehyde and 2,6-difluro benzaldehyde were purchased from Sigma-Aldrich (United Kingdom). 4-Hydroxy-1,1-dioxo-1,2-dihydro-1λ^6-benzo[*e*][1,2]thiazine-3-carboxylic acid methyl ester **3** and 1,1- dioxo-2,3-dihydro-1*H*-1λ^6-benzo[*e*][1,2]thiazin-4-one **4** were prepared following reported procedures [48, 49, 56, 57].

^{1}H and ^{13}C{^{1}H} (DEPTQ) NMR spectra were recorded on a Bruker Avance AVIII 400 MHz NMR spectrometers at ambient temperature. High resolution mass spectra data recorded on a Bruker micrOTOF-Q II mass spectrometer in positive electrospray ionization (ESI) mode. Thin layer chromatography (TLC) was performed on aluminum sheets pre-coated with Merck silica gel 60 F254 and detection was achieved under ultraviolet (UV) light.

General Procedure for the Synthesis of 5a–5o

Compound **4** (5.00 g, 25.4 mmol) was dissolved in methanol (50 mL) and aqueous NaOH (3.04 g, 76.1 mmol) was added to get a brownish yellow solution. Then a methanolic solution of the corresponding aldehyde was added dropwise and stirred at room temperature for 2 h. After completion of the reaction as monitored by TLC, acidified the reaction mixture with 10% HCl to get the yellowish precipitates, which was filtered, washed with water (3 × 25 mL) and recrystallised from methanol to obtain pure **5a-5o** [48, 49].

(Z)-3-Benzylidene-1,1-dioxo-2,3-dihydro-1H-1λ_6-benzo[e][1,2]thiazin-4-one, **5a**

Compound **5a** was synthesized following the general procedure using **4** (3.00 g, 15.21 mmol) and benzaldehyde (1.55 mL, 15.21 mmol). Yield: 68% (2.95 g, light yellow powder). MS (ESI^+): *m/z* $[M+Na]^+$ = Calcd. for $C_{15}H_{11}NNaO_3S$ 308.0357, obs: 308.0347. FT-IR (KBr, cm^{-1}): 3099 (NH), 1651 (C=O), 1570 (C=C), 1492 ($NH_{def.}$), 1446 ($CH_{def.}$), 1319, 1172 (SO_2). ^1H NMR (400.13 MHz, [d_6]DMSO, 25 ℃): δ = 10.72 (s, 1H, H-2), 8.15-8.13 (m, 1H, H-5), 8.03-8.01 (m, 2H, H-13, H-17), 7.96-7.88 (m, 3H, H-6, H-8, H-7), 7.67 (s, 1H, H-11), 7.55-7.48 (m, 3H, H-14, H-15, H-16) ppm. $^{13}C\{^1H\}$ NMR (100.61 MHz, [d_6]DMSO, 25 ℃): δ = 180.0 (C-4), 141.5 (C-3), 134.7 (C-6), 133.4 (C-7), 132.7 (C-12), 132.3 (C-11), 131.6 (C-10), 131.5 (C-14, C-16), 130.9 (C-15), 130.4 (C-9), 129.0 (C-5), 128.9 (C-13, C-17), 122.16 (C-8) ppm.

(Z)-3-(2-Methoxy-benzylidene)-1,1-dioxo-2,3-dihydro-1H-1λ_6-benzo[e][1,2]thiazin-4-one, **5b**

Compound **5b** was synthesized following the general procedure using **4** (3.00 g, 15.21 mmol) and 2-methoxybenzaldehyde (1.84 mL, 15.21 mmol). Yield: 73% (3.50 g, light orange powder). MS (ESI^+): *m/z* $[M+Na]^+$ = Calcd. for $C_{16}H_{13}NNaO_4S$ 338.0463, obs: 338.0496. FT-IR (KBr, cm^{-1}): 3230 (NH), 1670 (C=O), 1585 (C=C), 1463 ($CH_{def.}$), 1290, 1168 (SO_2). ^1H NMR (400.13 MHz, [d_6]DMSO, 25 ℃): δ = 10.61 (s, 1H, H-2), 8.19 (dd, $^3J_{(H17,H16)}$ = 8 Hz, $^4J_{(H17,H15)}$ = 2 Hz, 1H, H-17), 8.14-8.12 (m, 1H, H-5), 7.94-7.87 (m, 4H, H-11, H-6, H-8, H-7), 7.52-7.47 (m, 1H, H-15), 7.15-7.09 (m, 2H, H-16, H-14), 3.89 (s, 1H, H-18) ppm. $^{13}C\{^1H\}$ NMR (100.61 MHz, [d_6]DMSO, 25 ℃): δ = 180.0 (C-4), 158.7 (C-13), 141.5 (C-3), 134.7 (C-6), 133.4 (C-7), 132.7 (C-15), 131.3 (C-10), 130.5 (C-9), 130.3 (C-17), 129.0 (C-5), 126.2 (C-16), 122.1 (C-8), 121.0 (C-12), 120.5 (C-11), 111.7 (C-13), 55.9 (C-18) ppm.

(Z)-3-(3-Methoxy-benzylidene)-1,1-dioxo-2,3-dihydro-1H-1λ^6-benzo[e][1,2]thiazin-4-one, **5c**

Compound **5c** was synthesized following the general procedure using **4** (3.00 g, 15.21 mmol) and 3-methoxybenzaldehyde (1.86 mL, 15.21 mmol). Yield: 67% (3.21 g, light yellow powder). MS (ESI^+): *m/z* $[M+Na]^+$ = Calcd. for $C_{16}H_{13}NNaO_4S$ 338.0463, obs: 338.0458. FT-IR (KBr, cm^{-1}): 3128 (NH), 1658 (C=O), 1589 (C=C), 1454 ($CH_{def.}$), 1303, 1166 (SO_2). ^1H NMR (400.13 MHz, [d_6]DMSO, 25 ℃): δ = 10.74 (s, 1H, H-2), 8.15-8.12 (m, 1H, H-5), 7.97-7.88 (m, 3H, H-6, H-8, H-7), 7.64 (s, 1H, H-11), 7.60-7.59 (m, 2H, H-13, H-17), 7.10 (t, $^3J_{(H16,H17)}$ = 8Hz, 1H, H-16), 7.10-7.08

(m, 1H, H-15), 3.82 (s, 1H, H-18) ppm. $^{13}C\{^{1}H\}$ NMR (100.61 MHz, [d_6]DMSO, 25 ℃): δ = 180.0 (C-4), 159.3 (C-14), 141.3 (C-3), 134.7 (C-6), 133.8 (C-12), 133.4 (C-7), 132.1 (C-16), 131.7 (C-10), 130.4 (C-9), 129.9 (C-17), 129.0 (C-5), 123.9 (C-11), 122.1 (C-8), 116.7 (C-15), 116.5 (C-13), 55.3 (C-18) ppm.

(Z)-3-(4-Methoxy-benzylidene)-1,1-dioxo-2,3-dihydro-1H-1λ^6-benzo[e][1,2]thiazin-4-one, **5d**

Compound **5d** was synthesized following the general procedure using **4** (3.00 g, 15.21 mmol) and 4-methoxybenzaldehyde (1.85 mL, 15.21 mmol). Yield: 70% (3.36 g, light yellow crystalline solid). MS (ESI$^+$): *m/z* $[M+Na]^+$ = Calcd. for $C_{16}H_{13}NNaO_4S$ 338.0463, obs: 338.0458. FT-IR (KBr, cm^{-1}): 3196 (NH), 1664 (C=O), 1575 (C=C), 1508 ($CH_{def.}$), 1309, 1172 (SO_2). ^{1}H NMR (400.13 MHz, [d_6]DMSO, 25 ℃): δ = 10.48 (s, 1H, H-2), 8.14-8.11 (m, 1H, H-5), 8.05-8.02 (m, 2H, H-13, H-17), 7.94-7.86 (m, 3H, H-6, H-8, H-7), 7.66 (s, 1H, H-11), 7.11-7.09 (m, 2H, H-14, H-16), 3.85 (s, 1H, H-18) ppm. $^{13}C\{^{1}H\}$ NMR (100.61 MHz, [d_6]DMSO, 25 ℃): δ = 179.8 (C-4), 161.5 (C-15), 141.5 (C-3), 134.5 (C-6), 133.8 (C-13, C-17), 134.0 (C-7), 133.3 (C-11), 130.6 (C-9), 129.5 (C-10), 128.9 (C-5), 125.3 (C-12), 122.2 (C-8), 114.5 (C-14, C-16), 55.5 (C-18) ppm.

(Z)-3-(2-Bromo-benzylidene)-1,1-dioxo-2,3-dihydro-1H-1λ^6-benzo[e][1,2]thiazin-4-one, **5e**

Compound **5e** was synthesized following general procedure using **4** (3.00 g, 15.21 mmol) and 2-bromobenzaldehyde (1.78 mL, 15.21 mmol). Yield: 66% (3.66 g, light yellow powder). MS (ESI$^+$): *m/z* $[M+Na]^+$ = Calcd. for $C_{15}H_{10}BrNNaO_3S$ 385.9462, obs: 385.9458. FT-IR (KBr, cm^{-1}): 3156 (NH), 1638 (C=O), 1594 (C=C), 1435 ($CH_{def.}$), 1313, 1156 (SO_2). ^{1}H NMR (400.13 MHz, [d_6]DMSO, 25 ℃): δ = 10.91 (s, 1H, H-2), 8.16-8.11 (m, 2H, H-5, H-14), 7.99-7.89 (m, 3H, H-6, H-8, H-7), 7.79 (dd, $^3J_{(H17,H16)}$ = 8 Hz, $^4J_{(H17,H15)}$ = 1 Hz, 1H, H-17), 7.71 (s, 1H, H-11), 7.59-7.55 (m, 1H, H-16), 7.41 (td, $^3J_{(H15,H16)/(H15,H14)}$ = 8 Hz, $^4J_{(H15,H17)}$ = 2 Hz, 1H, H-15) ppm. $^{13}C\{^{1}H\}$ NMR (100.61 MHz, [d_6]DMSO, 25 ℃): δ = 179.9 (C-4), 141.4 (C-3), 135.0 (C-12), 133.5 (C-6), 133.3 (C-7), 133.2 (C-14), 132.3 (C-10), 131.9 (C-15), 131.3 (C-17), 130.2 (C-9), 129.1 (C-5), 128.6 (C-11), 128.0 (C-16), 125.7(C-13), 122.1 (C-8) ppm.

(Z)-3-(3-Bromo-benzylidene)-1,1-dioxo-2,3-dihydro-1H-1λ^6-benzo[e][1,2]thiazin-4-one, **5f**

Compound **5f** was synthesized following the general procedure using **4** (3.00 g, 15.21 mmol) and 3-bromobenzaldehyde (1.77 mL, 15.21 mmol). Yield: 64% (3.55 g, yellow powder). MS (ESI$^+$): *m/z* $[M+Na]^+$ = Calcd. for $C_{15}H_{10}BrNNaO_3S$ 385.9462, obs: 385.9454. FT-IR (KBr, cm^{-1}): 3186 (NH), 1660 (C=O), 1579 (C=C), 1469 ($CH_{def.}$), 1298, 1165 (SO_2). ^{1}H NMR (400.13 MHz, [d_6]DMSO, 25 ℃): δ = 10.89 (s, 1H, H-2), 8.21 (t, 1H, $^4J_{(H13,H15)/(H13,H17)}$ = 2 Hz, H-13), 8.14-8.12 (m, 1H, H-5), 7.99-7.89 (m, 4H, H-17, H-8, H-6, H-7), 7.70-7.68 (m, 1H, H-15), 7.62 (s, 1H, H-11), 7.50-7.46 (m, 1H, H-16) ppm. ^{13}C{^{1}H} NMR (100.61 MHz, [d_6]DMSO, 25 ℃): δ = 179.8 (C-4), 141.3 (C-3), 134.9 (C-12), 134.9 (C-6), 133.5 (C-7), 133.3 (C-13), 133.2 (C-15), 132.6 (C-10), 130.9 (C-17), 130.4 (C-16), 130.3 (C-9), 129.9 (C-11), 129.1 (C-5), 122.2 (C-8), 122.0 (C-14) ppm.

(Z)-3-(4-Bromo-benzylidene)-1,1-dioxo-2,3-dihydro-1H-1λ^6-benzo[e][1,2]thiazin-4-one, **5g**

Compound **5g** was synthesized following the general procedure using **4** (3.00 g, 15.21 mmol) and 4-bromobenzaldehyde (2.82 g, 15.21 mmol). Yield: 69% (3.82 g, light yellow solid). MS (ESI$^+$): *m/z* $[M+Na]^+$ = Calcd. for $C_{15}H_{10}BrNNaO_3S$ 385.9462, obs: 385.9457. FT-IR (KBr, cm^{-1}): 3059 (NH), 1655 (C=O), 1580 (C=C), 1485 ($CH_{def.}$), 1320, 1174 (SO_2). ^{1}H NMR (400.13 MHz, [d_6]DMSO, 25 ℃): δ = 10.76 (s, 1H, H-2), 8.14-8.12 (m, 1H, H-5), 7.95-7.88 (m, 5H, H-13, H-17, H-6, H-8, H-7), 7.75-7.73 (m, 2H, H-14, H-16), 7.62 (s, 1H, H-11) ppm. ^{13}C{^{1}H} NMR (100.61 MHz, [d_6]DMSO, 25 ℃): δ = 179.9 (C-4), 141.3 (C-3), 134.8 (C-6), 133.5 (C-7), 133.2 (C-14, C-16), 132.1 (C-10), 132.0 (C-13, C-17), 131.9 (C-12), 130.6 (C-11), 130.4 (C-9), 129.0 (C-5), 124.4 (C-15), 122.2 (C-8) ppm.

(Z)-3-(3-Chloro-benzylidene)-1,1-dioxo-2,3-dihydro-1H-1λ^6-benzo[e][1,2]thiazin-4-one, **5h**

Compound **5h** was synthesized following the general procedure using **4** (3.00 g, 15.21 mmol) and 3-chlorobenzaldehyde (2.14 g, 15.21 mmol). Yield: 73% (3.65 g, light yellow crystaline solid). MS (ESI$^+$): *m/z* $[M+Na]^+$ = Calcd. for $C_{15}H_{10}ClNNaO_3S$ 341.9967, obs: 341.9962. FT-IR (KBr, cm^{-1}): 3167 (NH), 1655 (C=O), 1578 (C=C), 1444 ($CH_{def.}$), 1375, 1166 (SO_2). ^{1}H NMR (400.13 MHz, [d_6]DMSO, 25 ℃): δ = 10.87

(s, 1H, H-2), 8.13 (d, $^{3}J_{(H5,H6)}$ = 8 Hz, 1H, H-5), 8.08 (s, 1H, H-13), 7.97-7.89 (m, 4H, H-17, H-6, H-8, H-7), 7.63 (s, 1H, H-11), 7.56-7.55 (m, 2H, H-15, H-16) ppm. $^{13}C\{^{1}H\}$ NMR (100.61 MHz, [d_6]DMSO, 25 ℃): δ = 179.8 (C-4), 141.3 (C-3), 134.9 (C-6), 134.7 (C-12), 133.5 (C-7), 133.4 (C-14), 132.6 (C-10), 130.7 (C-11), 130.03 (C-13), 130.4 (C-15), 130.2 (C-9), 130.2 (C-16), 130.1 (C-17), 129.0 (C-5), 122.2 (C-8) ppm.

(Z)-3-(4-Chloro-benzylidene)-1,1-dioxo-2,3-dihydro-1H-1λ^{6}-benzo[e][1,2]thiazin-4-one, **5i**

Compound **5i** was synthesized following the general procedure using **4** (3.00 g, 15.21 mmol) and 4-chlorobenzaldehyde (2.14 g, 15.21 mmol). Yield: 71% (3.45 g, yellow crystaline solid). MS (ESI^{+}): *m/z* $[M+Na]^{+}$ = Calcd. for $C_{15}H_{10}ClNNaO_3S$ 341.9967, obs: 341.9959. FT-IR (KBr, cm^{-1}): 3078 (NH), 1654 (C=O), 1577 (C=C), 1489 ($NH_{def.}$), 1400 ($CH_{def.}$), 1300, 1161 (SO_2). ^{1}H NMR (400.13 MHz, [d_6]DMSO, 25 ℃): δ = 10.76 (s, 1H, H-2), 8.14-8.12 (m, 1H, H-5), 8.04-8.02 (m, 2H, H-13, H-17), 7.96-7.89 (m, 3H, H-6, H-8, H-7), 7.65 (s, 1H, H-11), 7.62-7.59 (m, 2H, H-14, H-16) ppm. $^{13}C\{^{1}H\}$ NMR (100.61 MHz, [d_6]DMSO, 25 ℃): δ = 179.9 (C-4), 141.4 (C-3), 135.4 (C-15), 134.8 (C-6), 133.5 (C-7), 133.1 (C-14, C-16), 132.0 (C-12), 131.6 (C-10), 130.5 (C-11), 130.4 (C-9), 129.0 (C-11), 129.0 (C-13, C-17), 122.3 (C-8) ppm.

(Z)-3-(2,4-Dichloro-benzylidene)-1,1-dioxo-2,3-dihydro-1H-1λ^{6}-benzo[e][1,2]thiazin-4-one, **5j**

Compound **5j** was synthesized following the general procedure using **4** (3.00 g, 15.21 mmol) and 2,4-dichlorobenzaldehyde (2.7 g, 15.21 mmol). Yield: 67% (3.61 g, yellow crystaline solid). MS (ESI^{+}): *m/z* $[M+Na]^{+}$ = Calcd. for $C_{15}H_9Cl_2NNaO_3S$ 375.9578, obs: 375.9461. FT-IR (KBr): 3163 (NH), 1689 (C=O), 1600 (C=C), 1465 ($NH_{def.}$), 1392 ($CH_{def.}$), 1303, 1161 (SO_2). ^{1}H NMR (400.13 MHz, [d_6]DMSO, 25 ℃): δ = 10.98 (s, 1H, H-2), 8.17-8.13 (m, 2H, H-5, H-17), 7.99-7.89 (m, 3H, H-6,H-8, H-7), 7.81 (d, $^{4}J_{(H14,H16)}$ = 2 Hz, 1H, H-14), 7.67-7.64 (m, 2H, H-11, H-16) ppm. $^{13}C\{^{1}H\}$ NMR (100.61 MHz, [d_6]DMSO, 25 ℃): δ = 179.7 (C-4), 141.3 (C-3), 135.6 (C-15), 135.3 (C-13), 135.1 (C-6), 133.9 (C-12), 133.5 (C-7), 132.2 (C-11), 130.1 (C-10), 129.7 (C-9), 129.5 (C-17), 129.1 (C-5), 127.8 (C-16), 124.2 (C-14), 122.1 (C-8) ppm.

(Z)-3-(3-Fluoro-benzylidene)-1,1-dioxo-2,3-dihydro-1H-1λ^{6}-benzo[e][1,2]thiazin-4-one, **5k**

Compound **5k** was synthesized following the general procedure using **4** (3.00 g, 15.21 mmol) and 3-fluorobenzaldehyde (1.89 mL, 15.21 mmol). Yield: 85% (3.92 g, brownish yellow powder). MS (ESI^+): *m/z* $[M+Na]^+$ = Calcd. for $C_{15}H_{10}FNNaO_3S$ 326.0263, obs: 326.0257. FT-IR (KBr, cm^{-1}): 3116 (NH), 1685 (C=O), 1590 (C=C), 1448 ($CH_{def.}$), 1372, 1160 (SO_2). ^1H NMR (400.13 MHz, [d_6]DMSO, 25 ℃): δ = 10.85 (s, 1H, H-2), 8.15-8.13 (m, 1H, H-5), 7.96-7.82 (m, 4H, H-6, H-8, H-7, H-13, H-17), 7.65 (s, 1H, H-11), 7.59-7.54 (m, 1H, H-16), 7.38-7.32 (m, 1H, H-15) ppm. $^{13}C\{^1H\}$ NMR (100.61 MHz, [d_6]DMSO, 25 ℃): δ = 179.9 (C-4), 162.2 (d, $^1J_{(C,F)}$ = 243 Hz, C-14), 141.4 (C-3), 134.9 (C-6), 134.8 (C-10), 133.5 (C-7), 132.5 (C-12), 130.8 (d, $^3J_{(C,F)}$ = 8 Hz, C-16), 130.3 (C-9), 130.2 (C-17), 129.1 (C-5), 127.8 (d, $^4J_{(C,F)}$ = 2 Hz, C-11), 122.2 (C-8), 117.4 (d, $^2J_{(C,F)}$ = 23 Hz, C-15), 117.2 (d, $^2J_{(C,F)}$ = 23 Hz, C-13) ppm.

(Z)-3-(4-Fluoro-benzylidene)-1,1-dioxo-2,3-dihydro-1H-1λ^6-benzo[e][1,2]thiazin-4-one, **5l**

Compound **5l** was synthesized following the general procedure using **4** (3.00 g, 15.21 mmol) and 4-fluorobenzaldehyde (1.63 mL, 15.21 mmol). Yield: 75% (3.42 g, light yellow powder). MS (ESI^+): *m/z* $[M+Na]^+$ = Calcd. for $C_{15}H_{10}FNNaO_3S$ 326.0263, obs: 326.0259. FT-IR (KBr, cm^{-1}): 3187 (NH), 1661 (C=O), 1577 (C=C), 1443 ($CH_{def.}$), 1320, 1153 (SO_2). ^1H NMR (400.13 MHz, [d_6]DMSO, 25 ℃): δ = 10.69 (s, 1H, H-2), 8.14-8.09 (m, 3H, H-5, H-13, H-17), 7.96-7.88 (m, 3H, H-6,H-8, H-7), 7.68 (s, 1H, H-11), 7.41-7.36 (m, 2H, H-14, H-16) ppm. $^{13}C\{^1H\}$ NMR (100.61 MHz, [d_6]DMSO, 25 ℃): δ = 179.9 (C-4), 163.2 (d, $^1J_{(C,F)}$ = 252 Hz, C-15), 141.4 (C-3), 134.7 (C-6), 134.1 (C-13/C-17), 134.0 (C-13/C-17), 133.5 (C-7), 131.2 (C-10), 131.1 (C-11), 130.4 (C-9), 129.3 (C-12), 129.0 (C-5), 122.2 (C-8), 116.2 (C-14/C-16), 115.9 (C-14/C-16) ppm.

(Z)-3-(2,6-Difluoro-benzylidene)-1,1-dioxo-2,3-dihydro-1H-1λ^6-benzo[e][1,2]thiazin-4-one, **5m**

Compound **5m** was synthesized following the general procedure using **4** (3.00 g, 15.21 mmol) and 2,6-difluorobenzaldehyde (1.64 mL, 15.21 mmol). Yield: 76% (3.71 g, light yellow powder). MS (ESI^+): *m/z* $[M+Na]^+$ = Calcd. for $C_{15}H_9F_2NNaO_3S$ 344.0169, obs: 344.0163. FT-IR (KBr, cm^{-1}): 3085 (NH), 1655 (C=O), 1571 (C=C), 1490 ($NH_{def.}$), 1446 ($CH_{def.}$), 1319, 1170 (SO_2). ^1H NMR (400.13 MHz, [d_6]DMSO, 25

℃): δ = 11.03 (s, 1H, H-2), 8.14 (dd, $^{3}J_{(H5,H6)}$ = 7 Hz, $^{4}J_{(H5,H7)}$ = 2 Hz, 1H, H-5), 7.98-7.88 (m, 3H, H-6, H-8, H-7), 7.79-7.52 (m, 1H, H-15), 7.25-7.19 (m, 3H, H-11, H-14, H-16) ppm. $^{13}C\{^{1}H\}$ NMR (100.61 MHz, [d_6]DMSO, 25 ℃): δ = 179.0 (C-4), 161.2 (d, $^{3}J_{(C,F)}$ = 7 Hz, C-13/C-17), 158.8 (d, $^{3}J_{(C,F)}$ = 7 Hz, C-13/C-17), 141.6 (C-3), 135.9 (C-10), 135.0 (C-6), 133.3 (C-7), 132.1 (d, $^{2}J_{(C,F)}$ = 11 Hz, C-15), 130.1 (C-9), 129.1 (C-5), 121.6 (C-8), 114.4 (C-11), 112.1 (C-14), 111.9 (C-16), 130.4 (t, $^{2}J_{(C,F)}$ = 19 Hz, C-12) ppm.

(Z)-3-(2-Methyl-benzylidene)-1,1-dioxo-2,3-dihydro-1H-1λ^{6}-benzo[e][1,2]thiazin-4-one, **5n**

Compound **5n** was synthesized following the general procedure using **4** (3.00 g, 15.21 mmol) and 2-methylbenzaldehyde (1.76 mL, 15.12 mmol). Yield: 76% (3.46 g, light yellow crystaline solid). MS (ESI^{+}): *m/z* $[M+Na]^{+}$ = Calcd. for $C_{16}H_{13}NNaO_3S$ 322.0514, obs: 322.0504. FT-IR (KBr, cm^{-1}): 3176 (NH), 1666 (C=O), 1575 (C=C), 1458 ($CH_{def.}$), 1301, 1165 (SO_2). ^{1}H NMR (400.13 MHz, [d_6]DMSO, 25 ℃): δ = 10.66 (s, 1H, H-2), 8.14 (dd, $^{3}J_{(H5,H6)}$ = 8 Hz, $^{4}J_{(H5,H7)}$ = 1 Hz, 1H, H-5), 8.0-7.88 (m, 4H, H-17, H-6, H-8, H-7), 7.77 (s, 1H, H-11), 7.37-7.32 (m, 3H, H-15, H-16, H-14), 2.39 (s, 1H, H-18) ppm. $^{13}C\{^{1}H\}$ NMR (100.61 MHz, [d_6]DMSO, 25 ℃): δ = 180.1 (C-4), 141.5 (C-3), 138.9 (C-13), 134.8 (C-6), 133.4 (C-7), 132.1 (C-12), 131.5 (C-10), 130.6 (C-11), 130.4 (C-9), 130.2 (C-14), 129.6 (C-17), 129.4 (C-15), 129.0 (C-5), 126.3 (C-16), 122.1 (C-8), 19.7 (C-18) ppm.

(Z)-3-(3-Hydroxy-benzylidene)-1,1-dioxo-2,3-dihydro-1H-1λ^{6}-benzo[e][1,2]thiazin-4-one, **5o**

Compound **5o** was synthesized the following general procedure using **4** (3.00 g, 15.21 mmol) and 3-hydroxybenzaldehyde (1.86 g, 15.21 mmol). Yield: 63% (2.89 g, light yellow powder). MS (ESI^{+}): *m/z* $[M+Na]^{+}$ = Calcd. for $C_{15}H_{11}NNaO_4S$ 324.0306, obs: 324.0309. FT-IR (KBr, cm^{-1}): 3163 (NH), 3105-2725 (OH), 1637 (C=O), 1581 (C=C), 1450 ($CH_{def.}$), 1336, 1174 (SO_2). ^{1}H NMR (400.13 MHz, [d_6]DMSO, 25 ℃): δ = 10.64 (s, 1H, H-2), 9.75 (s, 1H, H-18), 8.12 (d, $^{3}J_{(H5,H6)}$= 8 Hz, 1H, H-5), 7.97-7.87 (m, 3H, H-6, H-8, H-7), 7.55-7.53 (s, 2H, H-11, H-13), 7.38-7.29 (m, 2H, H-15, H-16), 6.91 (dd, $^{3}J_{(H17,H16)}$ = 8 Hz, $^{4}J_{(H17,H15)}$ = 1 Hz, 1H, C-17) ppm. $^{13}C\{^{1}H\}$ NMR (100.61 MHz, [d_6]DMSO, 25 ℃): δ = 180.0 (C-4), 156.5 (C-14), 141.5 (C-3), 134.7 (C-6),

133.8 (C-12), 133.4 (C-7), 132.4 (C-11), 131.4 (C-10), 130.5 (C-9), 129.9 (C-16), 129.0 (C-5), 123.2 (C-17), 122.2 (C-8), 118.3 (C-13), 117.4 (C-15)ppm.

Cell transfection and preparation of membrane fractions

Plasmids expressing human alkaline phosphatases (h-TNAP & h-IAP) were transfected into COS-7 cells using lipofectamine following a published protocol [58, 59]. COS-7 cells at a confluence of 80-90% were incubated with 6 µg of plasmid DNA and 24 µL of lipofectamine reagent for 5 h at 37 ℃ in Dulbecco's modified Eagle's medium (DMEM) without fetal bovine serum (FBS). Transfection was stopped by adding the same volume of DMEM/F-12 containing 20% FBS. The cells were harvested 40 to 72 h later and were processed as reported [58]. Total protein was estimated using the Bradford test and different aliquotes of the protein were prepared with the addition of 7.5% glycerol and stored at -80 ℃ [60].

Inhibition of alkaline phosphatases *h*-TNAP and *h*-IAP

The inhibitory effect of the synthesized derivatives on *h*-TNAP and *h*-IAP was determined at concentrations of up to 200 µM, using a method reported previously [13, 61]. The solutions were prepared in buffer containing 3 M DEA (pH 9.8), 2.5 mM $MgCl_2$ and 0.05 mM $ZnCl_2$. The compound samples (0.2 mM) were prepared in an aqueous solution with a final DMSO content of 1% (v/v) and 10 µL of that solution was mixed with 20 µL of a solution of *h*-TNAP (46 ng/well) or *h*-IAP (57 ng/well) cell lysates in 384-well plates. The luminescence signals were recorded with a microplate reader (BioTek FLx800, Instruments, Inc. USA) after incubating the plates at 37 ℃ for 5–10 min. Then, CDP-star® substrate (2 0 µL; disodium 2-chloro-5-(4-methoxyspiro[1,2-dioxetane-3,2′-(5-chlorotricyclo[3.3.1.13.7]decan])-4-yl]-1-phenyl phosphate) was added and the luminescence was again measured after 15–20 min of incubation. The data was evaluated with PRISM 5.0 (GraphPad, San Diego, California, USA) software and the inhibitory concentration values at 50% inhibition (IC_{50} values) were obtained [61].

Molecular docking studies

The binding interactions of the most effective derivatives **5c** and **5i** within the respective enzymes i.e., h-IAP and h-TNAP were studied with molecular docking using modelled structures [13, 62]. For docking studies the chemical structure of potent compounds were 3D optimized using ACD/Chem Sketch software. Energy minimization and protonation of targeted proteins structures were carried out by using Molecular Operating Environment (MOE 2014.009) software [63], as discussed previously [13]. After the docking calculations, the configurations with the lowest binding free energy were selected and further analyzed with Discovery Studio Visualizer to determine their probable binding modes within the active site of the target enzymes.

Cell Viability Assay (MTT Assay)

The antiproliferative effect of **5a–5o** was investigated against HeLa cells with the MTT assay following a reported protocol [64, 65]. Briefly, 90 µL of the cell culture medium containing 2.5 × 10^4 cells/mL was seeded overnight in 96-well plates. Then, 10 µL (final concentration of 100 µM) of the test compound was added, followed by an incubation for 24 h at 37 ℃. Cisplatin (final c oncentration of 100 µM) was used as reference drug while medium was used as the negative control. After 24 h, 10 µL of MTT reagent (final concentration of 5 µg/well) was added to each well and incubated for 4 h at 37 ℃. The MTT activity on the cells was stopped by adding 100 µL/well of an aqueous solution of 50% isopropanol and 10% sodium dodecyl sulfate, followed by gentle agitation (for 30 minutes) at room temperature. The optical density was measured using a microplate reader (Bio-Tek ELx 800^{TM}, Instruments, Inc. Winooski, VT, USA) at 570 nm along with the background at 690 nm. All experiments were performed in triplicate. Results reported are means of three independent experiments (± SEM) and expressed as percent inhibitions calculated by the equation

$$Inhibition\ (\%) = 100 - \frac{absorbance\ of\ the\ test\ compounds}{absorbance\ of\ the\ control} \times 100$$

References

[1] M. Haarhaus, V. Brandenburg, K. Kalantar-Zadeh, P. Stenvinkel, P. Magnusson, Alkaline phosphatase: a novel treatment target for cardiovascular disease in CKD, Nat. Rev. Nephrol., 13 (2017) 429-442.

[2] M.H. Le Du, J.L. Millan, Structural evidence of functional divergence in human alkaline phosphatases, J. Biol. Chem., 277 (2002) 49808-49814.

[3] P. Llinas, E.A. Stura, A. Menez, Z. Kiss, T. Stigbrand, J.L. Millan, M.H. Le Du, Structural studies of human placental alkaline phosphatase in complex with functional ligands, J. Mol. Biol., 350 (2005) 441-451.

[4] U. Sharma, D. Pal, R. Prasad, Alkaline phosphatase: an overview, Indian J. Clin. Biochem., 29 (2014) 269-278.

[5] D. Harmey, L. Hessle, S. Narisawa, K.A. Johnson, R. Terkeltaub, J.L. Millan, Concerted regulation of inorganic pyrophosphate and osteopontin by Akp2, Enpp1, and Ank - An integrated model of the pathogenesis of mineralization disorders, Am. J. Pathol., 164 (2004) 1199-1209.

[6] X.J. Tian, X.H. Song, S.L. Yan, Y.X. Zhang, H.M. Zhou, Study of refolding of calf intestinal alkaline phosphatase, J. Protein Chem., 22 (2003) 417-422.

[7] T. Malati, Tumour markers: An overview, Indian J. Clin. Biochem., 22 (2007) 17-31.

[8] J.L. Millán, Neoplastic Expression of PLAP, GCAP, IAP (Regan, Nagao, Kasahara) and TNAP Isozymes, in: Mammalian Alkaline Phosphatases, Wiley-VCH Verlag GmbH & Co. KGaA, Weinheim, 2006, pp. 187-205.

[9] J.L. Millán, APs as Physiological and Disease Markers, in: Mammalian Alkaline Phosphatases, Wiley-VCH Verlag GmbH & Co. KGaA, Weinheim, 2006, pp. 165-185.

[10] J.L. Millán, APs as Therapeutic Agents, in: Mammalian Alkaline Phosphatases, Wiley-VCH Verlag GmbH & Co. KGaA, Weinheim, 2006, pp. 227-236.

[11] W.H. Fishman, N.I. Inglis, S. Green, L-Phenylalanine - an Organ Specific, Stereospecific Inhibitor of Human Intestinal Alkaline Phosphatase, Nature, 198 (1963) 685-686.

[12] S. Narisawa, D. Harmey, M.C. Yadav, W.C. O'Neill, M.F. Hoylaerts, J.L. Millan, Novel inhibitors of alkaline phosphatase suppress vascular smooth muscle cell calcification, J. Bone Miner. Res., 22 (2007) 1700-1710.

[13] I. Khan, A. Ibrar, S.A. Ejaz, S.U. Khan, S.J.A. Shah, S. Hameed, J. Simpson, J. Lecka, J. Sévigny, J. Iqbal, Influence of the diversified structural variations at the imine functionality of 4-bromophenylacetic acid derived hydrazones on alkaline phosphatase inhibition: synthesis and molecular modelling studies, RSC Advances, 5 (2015) 90806-90818.

[14] M. al-Rashida, S.A. Ejaz, S. Ali, A. Shaukat, M. Hamayoun, M. Ahmed, J. Iqbal, Diarylsulfonamides and their bioisosteres as dual inhibitors of alkaline phosphatase and carbonic anhydrase: Structure activity relationship and molecular modelling studies, Bioorg. Med. Chem., 23 (2015) 2435-2444.

[15] M. Miliutina, S.A. Ejaz, V.O. Iaroshenko, A. Villinger, J. Iqbal, P. Langer, Synthesis of 3,3'-carbonyl-bis(chromones) and their activity as mammalian alkaline phosphatase inhibitors, Org. Biomol. Chem., 14 (2016) 495-502.

[16] S.A. Ejaz, A. Saeed, M.N. Siddique, Z.U. Nisa, S. Khan, J. Lecka, J. Sévigny, J. Iqbal, Synthesis, characterization and biological evaluation of novel chalcone sulfonamide hybrids as potent intestinal alkaline phosphatase inhibitors, Bioorg. Chem., 70 (2017) 229-236.

[17] C.L. Zhuang, W. Zhang, C.Q. Sheng, W.N. Zhang, C.G. Xing, Z.Y. Miao, Chalcone: A Privileged Structure in Medicinal Chemistry, Chem. Rev., 117 (2017) 7762-7810.

[18] H. Wei, J.L. Ruan, X.J. Zhang, Coumarin-chalcone hybrids: promising agents with diverse pharmacological properties, RSC Adv., 6 (2016) 10846-10860.

[19] L.M. Ni, C.Q. Meng, J.A. Sikorski, Recent advances in therapeutic chalcones, Expert Opin. Therap. Pat., 14 (2004) 1669-1691.

[20] Z. Nowakowska, A review of anti-infective and anti-inflammatory chalcones, Eur. J. Med. Chem., 42 (2007) 125-137.

[21] E.B. Yang, Y.J. Guo, K. Zhang, Y.Z. Chen, P. Mack, Inhibition of epidermal growth factor receptor tyrosine kinase by chalcone derivatives, Biochim. Biophys. Acta, Protein Struct. Mol. Enzymol., 1550 (2001) 144-152.

[22] S.U.F. Rizvi, H.L. Siddiqui, M. Nisar, N. Khan, I. Khan, Discovery and molecular docking of quinolyl-thienyl chalcones as anti-angiogenic agents targeting VEGFR-2 tyrosine kinase, Bioorg. Med. Chem. Lett., 22 (2012) 942-944.

[23] B. Srinivasan, T.E. Johnson, R. Lad, C. Xing, Structure-activity relationship studies of chalcone leading to 3-hydroxy-4,3',4',5'-tetramethoxychalcone and its

analogues as potent nuclear factor kappaB inhibitors and their anticancer activities, J. Med. Chem., 52 (2009) 7228-7235.

[24] H. Mirzaei, S. Emami, Recent advances of cytotoxic chalconoids targeting tubulin polymerization: Synthesis and biological activity, Eur. J. Med. Chem., 121 (2016) 610-639.

[25] B.X. Zhang, D.Z. Duan, C.P. Ge, J. Yao, Y.P. Liu, X.M. Li, J.G. Fang, Synthesis of Xanthohumol Analogues and Discovery of Potent Thioredoxin Reductase Inhibitor as Potential Anticancer Agent, J. Med. Chem., 58 (2015) 1795-1805.

[26] H.L. Ng, X. Ma, E.H. Chew, W.K. Chui, Design, Synthesis, and Biological Evaluation of Coupled Bioactive Scaffolds as Potential Anticancer Agents for Dual Targeting of Dihydrofolate Reductase and Thioredoxin Reductase, J. Med. Chem., 60 (2017) 1734-1745.

[27] F. Lovering, J. Bikker, C. Humblet, Escape from Flatland: Increasing Saturation as an Approach to Improving Clinical Success, J. Med. Chem., 52 (2009) 6752-6756.

[28] F. Aman, M. Hanif, W.A. Siddiqui, A. Ashraf, L.K. Filak, J. Reynisson, T. Sohnel, S.M.F. Jamieson, C.G. Hartinger, Anticancer Ruthenium(eta(6)-p-cymene) Complexes of Nonsteroidal Anti-inflammatory Drug Derivatives, Organometallics, 33 (2014) 5546-5553.

[29] F. Aman, M. Hanif, M. Kubanik, A. Ashraf, T. Sohnel, S.M.F. Jamieson, W.A. Siddiqui, C.G. Hartinger, Anti-Inflammatory Oxicams as Multi-donor Ligand Systems: pH- and Solvent-Dependent Coordination Modes of Meloxicam and Piroxicam to Ru and Os, Chem. Eur. J., 23 (2017) 4893-4902.

[30] N. Ahmad, M. Zia-ur-Rehman, H.L. Siddiqui, M.F. Ullah, M. Parvez, Microwave assisted synthesis and structure-activity relationship of 4-hydroxy-*N*'-[1-phenylethylidene]-2*H*/2-methyl-1,2-benzothiazine-3-carbohydrazide 1,1-dioxides as anti-microbial agents, Eur J Med Chem, 46 (2011) 2368-2377.

[31] M.L. Barreca, G. Manfroni, P. Leyssen, J. Winquist, N. Kaushik-Basu, J. Paeshuyse, R. Krishnan, N. Iraci, S. Sabatini, O. Tabarrini, A. Basu, U.H. Danielson, J. Neyts, V. Cecchetti, Structure-Based Discovery of Pyrazolobenzothiazine Derivatives As Inhibitors of Hepatitis C Virus Replication, J. Med. Chem., 56 (2013) 2270-2282.

[32] G. Manfroni, D. Manvar, M.L. Barreca, N. Kaushik-Basu, P. Leyssen, J. Paeshuyse, R. Cannalire, N. Iraci, A. Basu, M. Chudaev, C. Zamperini, E. Dreassi, S. Sabatini, O. Tabarrini, J. Neyts, V. Cecchetti, New Pyrazolobenzothiazine

Derivatives as Hepatitis C Virus NS5B Polymerase Palm Site I Inhibitors, J. Med. Chem., 57 (2014) 3247-3262.

[33] N. Ahmad, M. Zia-ur-Rehman, H.L. Siddiqui, M.F. Ullah, M. Parvez, Microwave assisted synthesis and structure-activity relationship of 4-hydroxy-N '-[1-phenylethylidene]-2H/2-methyl-1,2-benzothiazine-3-carbohydrazide 1,1-dioxides as anti-microbial agents, Eur J Med Chem, 46 (2011) 2368-2377.

[34] M. Zia-Ur-Rehman, J.A. Choudary, M.R.J. Elsegood, H.L. Siddiqui, K.M. Khan, A facile synthesis of novel biologically active 4-hydroxy-*N*'-(benzylidene)-2*H*-benzo[*e*][1,2]thiazine-3-carbohydrazide 1,1-dioxides, Eur. J. Med. Chem., 44 (2009) 1311-1316.

[35] M. Ahmad, H.L. Siddiqui, M. Zia-Ur-Rehman, M. Parvez, Anti-oxidant and anti-bacterial activities of novel *N*'-arylmethylidene-2-(3, 4-dimethyl-5, 5-dioxidopyrazolo[4,3-*c*][1,2]benzothiazin-2(4*H*)-yl) acetohydrazides, Eur. J. Med. Chem., 45 (2010) 698-704.

[36] Y. Tasaki, J. Yamamoto, T. Omura, T. Noda, N. Kamiyama, K. Yoshida, M. Satomi, T. Sakaguchi, M. Asari, T. Ohkubo, K. Shimizu, K. Matsubara, Oxicam structure in non-steroidal anti-inflammatory drugs is essential to exhibit Akt-mediated neuroprotection against 1-methyl-4-phenyl pyridinium-induced cytotoxicity, Eur. J. Pharmacol., 676 (2012) 57-63.

[37] A. Ashraf, M. Kubanik, F. Aman, H. Holtkamp, T. Sohnel, S.M.F. Jamieson, M. Hanif, W.A. Siddiqui, C.G. Hartinger, Ru-II(eta(6)-p-cymene) Complexes of Bioactive 1,2-Benzothiazines: Protein Binding vs. Antitumor Activity, Eur. J. Inorg. Chem., (2016) 1376-1382.

[38] S.H. Kim, R. Ramu, S.W. Kwon, S.H. Lee, C.H. Kim, S.K. Kang, S.D. Rhee, M.A. Bae, S.H. Ahn, D.C. Ha, H.G. Cheon, K.Y. Kim, J.H. Ahn, Discovery of cyclicsulfonamide derivatives as 11 beta-hydroxysteroid dehydrogenase 1 inhibitors, Bioorg. Med. Chem. Lett., 20 (2010) 1065-1069.

[39] G.J. Wells, M. Tao, K.A. Josef, R. Bihovsky, 1,2-Benzothiazine 1,1-dioxide P(2)-P(3) peptide mimetic aldehyde calpain I inhibitors, J. Med. Chem., 44 (2001) 3488-3503.

[40] X. Chen, S.Z. Zhang, Y.C. Yang, S. Hussain, M.L. He, D.Q. Gui, B. Ma, C.J. Jing, Z.X. Qiao, C.J. Zhu, Q. Yu, 1,2-Benzothiazine 1,1-dioxide carboxylate derivatives as novel potent inhibitors of aldose reductase, Bioorg. Med. Chem., 19 (2011) 7262-7269.

[41] X. Chen, C.J. Zhu, F. Guo, X.W. Qiu, Y.C. Yang, S.Z. Zhang, M.L. He, S. Parveen, C.J. Jing, Y. Li, B. Ma, Acetic Acid Derivatives of 3,4-Dihydro-2*H*-1,2,4-benzothiadiazine 1,1-Dioxide as a Novel Class of Potent Aldose Reductase Inhibitors, J. Med. Chem., 53 (2010) 8330-8344.

[42] S. Parveen, S. Hussain, S.J. Zhu, X.Y. Qin, X. Hao, S.Z. Zhang, J.L. Lu, C.J. Zhu, Selective synthesis and comparative activity of olefinic isomers of 1,2-benzothiazine-1,1-dioxide carboxylates as aldose reductase inhibitors, RSC Adv., 4 (2014) 21134-21140.

[43] Y. Cheng, C. Bolm, Regioselective Syntheses of 1,2-Benzothiazines by Rhodium-Catalyzed Annulation Reactions, Angew. Chem. Int. Edit., 54 (2015) 12349-12352.

[44] W.H. Jeon, J.Y. Son, J.E. Kim, P.H. Lee, Synthesis of 1,2-Benzothiazines by a Rhodium-Catalyzed Domino C-H Activation/Cyclization/Elimination Process from S-Aryl Sulfoximines and Pyridotriazoles, Org. Lett., 18 (2016) 3498-3501.

[45] J. Wen, D.P. Tiwari, C. Bolm, 1,2-Benzothiazines from Sulfoximines and Allyl Methyl Carbonate by Rhodium-Catalyzed Cross-Coupling and Oxidative Cyclization, Org. Lett., 19 (2017) 1706-1709.

[46] G.H. Ko, J.Y. Son, H. Kim, C. Maeng, Y. Baek, B. Seo, K. Um, P.H. Lee, Synthesis of Indolo-1,2-Benzothiazines from Sulfoximines and 3-Diazoindolin-2-imines, Adv. Synth. Catal., 359 (2017) 3362-3370.

[47] A. Ashraf, W.A. Siddiqui, J. Akbar, G. Mustafa, H. Krautscheid, N. Ullah, B. Mirza, F. Sher, M. Hanif, C.G. Hartinger, Metal complexes of benzimidazole derived sulfonamide: Synthesis, molecular structures and antimicrobial activity, Inorg. Chim. Acta, 443 (2016) 179-185.

[48] H. Zinnes, R.A. Comes, F.R. Zuleski, A.N. Caro, J. Shavel, 1,2-Benzothiazines .2. Preparation and Sodium Borohydride Reduction of 3-Acyl-2h-1,2-Benzothiazin-4(3h)-One 1,1-Dioxides, J. Org. Chem., 30 (1965) 2241-2246.

[49] H. Zinnes, R.A. Comes, J. Shavel, 1,2-Benzothiazines .3. Preparation of 2h-1,2-Benzothiazin-4(3h)-1 1,1-Dioxide by Acid-Catalyzed Deacetylation of Beta-Diketone, J. Org. Chem., 31 (1966) 162-165.

[50] J.G. Lombardi, E.H. Wiseman, W.M. Mclamore, Synthesis and Antiinflammatory Activity of Some 3-Carboxamides of 2-Alkyl-4-Hydroxy-2h-1,2-Benzothiazine 1,1-Dioxide, J. Med. Chem., 14 (1971) 1171-1175.

[51] C.B. Schapira, I.A. Perillo, S. Lamdan, 3-Oxo-1,2-Benzoisothiazoline-2-Acetic Acid 1,1-Dioxide Derivatives .1. Reaction of Esters with Alkoxides, J. Heterocycl. Chem., 17 (1980) 1281-1288.

[52] M. Shafiq, I.U. Khan, M. Zia-ur-Rehman, M.N. Arshad, A.M. Asiri, 4-Hydrazinylidene-1-methyl-3H-2 lambda(6),1-benzothiazine-2,2-dione, Acta Crystallogr. E, 67 (2011) O2038-U2527.

[53] M.N. Arshad, O. Sahin, M. Zia-ur-Rehman, I.U. Khan, A.M. Asiri, H.M. Rafique, 4-hydroxy-2H-1,2-benzothiazine-3-carbohydrazide 1,1-dioxide-oxalohydrazide (1:1): X-ray structure and DFT calculations, J. Struct. Chem., 54 (2013) 437-442.

[54] M.N. Arshad, A.M. Asiri, K.A. Alamry, T. Mahmood, M.A. Gilani, K. Ayub, A.S. Birinji, Synthesis, crystal structure, spectroscopic and density functional theory (DFT) study of N-[3-anthracen-9-yl-1-(4-bromo-phenyl)-allylidene]-N-benzenesulfonohydrazine, Spectrochim. Acta A, 142 (2015) 364-374.

[55] E.A. Sergienko, J.L. Millán, High-throughput screening of tissue-nonspecific alkaline phosphatase for identification of effectors with diverse modes of action, Nat. Protoc., 5 (2010) 1431-1439.

[56] C.R. Rasmussen, D.L. Shaw, 3-Acyl-4-Hydroxy-2h-1,2-Benzothiazine 1,1-Dioxides .2. Reaction with Aziridines - Nucleophilic Displacements on (1,2,3,4-Tetrahydro-11-Hydroxy-1-Oxopyrazino[1,2-B][1,2]Benzothiazin-2-Yl)Ethyl Methanesulfonate 6,6-Dioxide, J. Org. Chem., 39 (1974) 1560-1563.

[57] C.R. Rasmussen, 3-Acyl-4-Hydroxy-2h-1,2-Benzothiazine 1,1-Dioxides .1. Alkylation, Amination, and Ethoxycarbonylation, J. Org. Chem., 39 (1974) 1554-1560.

[58] F. Kukulski, S.A. Levesque, E.G. Lavoie, J. Lecka, F. Bigonnesse, A.F. Knowles, S.C. Robson, T.L. Kirley, J. Sévigny, Comparative hydrolysis of P2 receptor agonists by NTPDases 1, 2, 3 and 8, Purinergic Signal., 1 (2005) 193-204.

[59] T. Kiffer-Moreira, C.R. Sheen, K.C.D. Gasque, M. Bolean, P. Ciancaglini, A. van Elsas, M.F. Hoylaerts, J.L. Millán, Catalytic Signature of a Heat-Stable, Chimeric Human Alkaline Phosphatase with Therapeutic Potential, Plos One, 9 (2014) 1-14.

[60] M.M. Bradford, A rapid and sensitive method for the quantitation of microgram quantities of protein utilizing the principle of protein-dye binding, Anal. Biochem., 72 (1976) 248-254.

[61] E. Sergienko, Y. Su, X. Chan, B. Brown, A. Hurder, S. Narisawa, J.L. Millán, Identification and Characterization of Novel Tissue-Nonspecific Alkaline

Phosphatase Inhibitors with Diverse Modes of Action, J. Biomol. Screen., 14 (2009) 824-837.

[62] I. Khan, S.J.A. Shah, S.A. Ejaz, A. Ibrar, S. Hameed, J. Lecka, J.L. Millán, J. Sévigny, J. Iqbal, Investigation of quinoline-4-carboxylic acid as a highly potent scaffold for the development of alkaline phosphatase inhibitors: synthesis, SAR analysis and molecular modelling studies, RSC Adv., 5 (2015) 64404-64413.

[63] Molecular Operating Environment (MOE), 2013.08; Chemical Computing Group ULC, 1010, Sherbooke St. West, Suite #910, Montreal, QC, Canada, H3A 2R7, 2018.

[64] T. Mosmann, Rapid colorimetric assay for cellular growth and survival: application to proliferation and cytotoxicity assays, J. Immunol. Methods, 65 (1983) 55-63.

[65] M. Niks, M. Otto, Towards an optimized MTT assay, J. Immunol. Methods, 130 (1990) 149-151.

Highlights

- synthesis of hybride compounds derived from chalcone and 1,2-benzothiazine pharmacophores
- potent and/or selective inhibitors of alkaline phosphatase isozymes
- structure-activity and selectivity study with regard to different substituents at the phenyl residue
- molecular docking studies of the most effective inhibitors of h-TNAP and h-IAP